

Crystallographic and Infrared Spectral Investigations of Mg^{2+} Substituted Cobalt Ferrite Nanoparticles Prepared by Sol-Gel Auto Combustion Technique

Vithal Vinayak Dhole¹, Pankaj P. Khirade², C. M. Kale³, V. G. Patil², N. D. Shinde², K. M. Jadhav^{2*}

¹ Department of Chemistry, B. S. S. Arts & Science College, Makni, Tq: Lohara, Osmanabad, Maharashtra, India.

² Department of Physics, Dr. Babasaheb Ambedkar Marathwada University, Aurangabad, Maharashtra, India.

³ Department of Physics, Indraraj Arts, Commerce and Science College Sillod, Aurangabad, Maharashtra, India.

Abstract

The present work focuses on the effect of magnesium (Mg^{2+}) substitution on structural, microstructural and infrared studies of the nanocrystalline cobalt ferrite ($CoFe_2O_4$). The samples of $Co_{1-x}Mg_xFe_2O_4$ nanocrystalline spinel ferrite of different compositions with $x = 0.0$ and 0.25 have been synthesized by sol-gel auto combustion method using citric acid ($C_6H_8O_7$) as a fuel; the prepared samples were sintered at $550\text{ }^\circ\text{C}$ for 4 h. The structural properties were estimated from X-ray diffraction (XRD) and Fourier Transform Infrared Spectroscopy (FTIR) studies. The microstructural studies were investigated through Scanning electron microscopy (SEM) technique. The average particle size was calculated by using Debye Scherer's formula using XRD data and is obtained to be 12-32 nm. The average grain size was found to be in nanometer range and of the order of 45-66 nm obtained by using SEM images. The IR spectra show two principle absorption bands in the range of 400 cm^{-1} to 1000 cm^{-1} .

Keywords: nanocrystalline, cobalt ferrite, sol-gel, XRD, SEM, FTIR.

1. Introduction

In recent years, spinel ferrites have been investigated for their useful magnetic properties and applications in information storage systems, sensors, actuators, magnetic fluids, microwave absorbers and medical diagnostics [1-6]. Thus much attention has been focused on the preparation and characterization of nanoparticles of spinel ferrites. Many important properties of the spinel ferrites crucially depend on the exact nature of the cation distribution. The nanoparticles are of three dimensional inorganic solids with diameter of the order of a nanometer (nm). It has been established that the unusual properties of the nanoferrites can be explained on the basis of the method of preparation, nature and type of substituent, particle size, pH, sintering temperature, etc. All these parameters can play a crucial role in the modification of the electrical and magnetic

properties of spinel ferrites which can be useful for the desired applications.

For the applications of nanomaterials in various diverse fields [7-9], it is necessary to be designed and exploited new materials of more predictable properties than what are currently available. Cobalt ferrite ($CoFe_2O_4$), owing to strong ferromagnetism and high Curie temperature, is used in electronic appliances since it stays magnetized even when the applied magnetic field is removed. This leads towards a useful way of information storage.

Co-Mg nano-ferrite is an interesting material because of its high coercivity, moderate saturation magnetization, good chemical stability and mechanical hardness; therefore it can found applications in magnetic drug delivery and high density information storage [10, 11].

The most widely used wet chemical method for the synthesis of spinel nanoferrites is the sol-gel auto combustion method. This method has several advantages over the other synthesis methods due to its low processing temperature, high chemical homogeneity, the possibility of controlling the size and morphology of particles etc.

Cobalt ferrite ($CoFe_2O_4$) with high magnetocrystalline anisotropy, high saturation magnetization, high electrical resistivity, high coercivity is one of the best candidate among the other spinel ferrite for various applications. Cobalt ferrite can be used in many applications such as magnetic drug delivery, microwave devices, high density information storage, ferro-fluids etc [12, 13].

The substitution of Zn, Ni ions in cobalt ferrite has led the modification in the properties of cobalt ferrite [14, 15]. Like Zn, magnesium (Mg) is also a nonmagnetic and can modify the properties of cobalt ferrite when substituted.

Thus, it will be interesting to study the structural, electrical and magnetic properties of Mg substituted cobalt ferrite ($Co_{1-x}Mg_xFe_2O_4$) nanoparticles. The aim of the present work is to study the structural and microstructural properties of $Co_{1-x}Mg_xFe_2O_4$ (for $x = 0.0$ and 0.25).

2. Experimental

2.1 Preparation of $\text{Co}_{1-x}\text{Mg}_x\text{Fe}_2\text{O}_4$ Spinel Ferrite Nanoparticles

The nanocrystalline samples of magnesium substituted cobalt ferrite ($\text{Co}_{1-x}\text{Mg}_x\text{Fe}_2\text{O}_4$, $x = 0$ and 0.25) were prepared using sol-gel auto combustion method. AR grade chemicals such as cobalt nitrate ($\text{Co}(\text{NO}_3)_2$), magnesium nitrate ($\text{Mg}(\text{NO}_3)_2$), ferric nitrate ($\text{Fe}(\text{NO}_3)_3$) and citric acid ($\text{C}_6\text{H}_8\text{O}_7$) were used for the synthesis. The metal nitrates to fuel (citric acid) ratio was taken as 1:3. Ammonia solution was added to maintain the pH 7. The temperature required for the synthesis of Co-Mg nanoparticles was low that is around 110°C . The as-synthesized powder is sintered at 550°C for 4 h and then used for further investigations of structural properties.

2.2 Characterizations

X-ray diffraction (XRD) technique was employed to characterize the prepared Co-Mg nanoparticles using REGAKU X-ray diffractometer. The XRD patterns were recorded at room temperature in the 2θ range of 20° to 80° using $\text{Cu-K}\alpha$ radiation ($\lambda = 1.54056 \text{ \AA}$). To investigate the chemical and structural Fourier transform infrared spectroscopy (FTIR) spectra of all the calcined samples were recorded in the range of $4000\text{-}450 \text{ cm}^{-1}$ IR-BRUKER-TENSOR 37-FTIR- ATR instrument. Morphology of the prepared samples was studied using Scanning electron microscope (SEM) JEOL-JSM 840 Model.

3. Results and Discussions

3.1 X-ray diffraction (XRD)

The X-ray diffraction patterns of the $\text{Co}_{1-x}\text{Mg}_x\text{Fe}_2\text{O}_4$ ($x = 0.0$ and 0.25) spinel ferrite nanoparticles are shown in fig.1 (a) and (b) respectively.

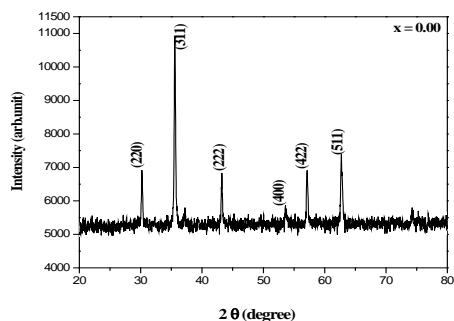


Fig. 1(a): XRD pattern of $\text{Co}_{1-x}\text{Mg}_x\text{Fe}_2\text{O}_4$ ($x = 0.00$)

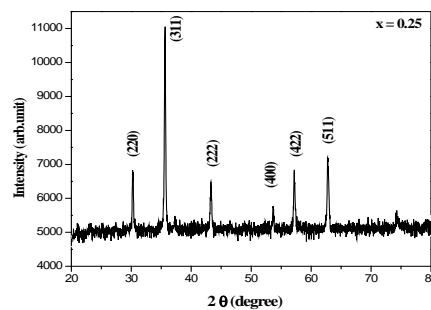


Fig. 1 (b): XRD pattern of $\text{Co}_{1-x}\text{Mg}_x\text{Fe}_2\text{O}_4$ ($x = 0.25$)

The both XRD patterns show the reflections belonging to cubic spinel structure; no extra peaks have been observed in the XRD patterns. The single phase formations of compounds under investigations were confirmed from the analysis of XRD pattern. The intensity of (311) plane is more as compared to other planes like (220), (222), (400), (422), (511) and (440) and is chosen for the determination of crystallite size.

Using the inter planar spacing (d) and the corresponding Miller indices, the lattice constant (a) of all the samples were calculated using standard relation,

$$a = d\sqrt{(h^2+k^2+l^2)} \quad \dots(1)$$

where, d is interplanar spacing and ($h k l$) are Miller Indices.

The obtained values of the lattice constant ' a ' are given in table 1. It is found that the lattice constant decreases with increase in magnesium content x . The decrease in lattice constant is attributed to the difference in the ionic radii of Co^{2+} and Mg^{2+} . The slight variation in lattice constant may be due to slight difference in the ionic radii of Co^{2+} (0.74 \AA) and Mg^{2+} (0.72 \AA) ions.

The unit cell volume (V) for both the samples was calculated by using the following equation and is represented in table 1.

$$V = a^3 \quad \dots(2)$$

where, V is the unit cell volume and a is the lattice constant.

The unit cell volume (V) shows gradual decrease with the substitution of magnesium for cobalt in the present ferrite system. The decrease in cell volume is attributed to decrease in lattice constant of the system under investigation.

The values of lattice constant and molecular weight were used to determine the X-ray density for all the samples. By using the following relation [16], the X-ray density was calculated

$$d_x = \frac{Z \times M}{V \times N_A} \quad \dots(3)$$

where, d_x is X-ray density, Z is the number of molecules per unit, M is molecular mass of the sample, V is the unit cell volume and N_A is the Avogadro's number.

Similar to lattice constant the X-ray density also decreases with increase in magnesium content x . The decrease in X-ray density is attributed to the decrease in mass overtakes the decrease in volume. Also due to difference in their atomic weight ($Co = 58.933$ a.m.u. and $Mg = 24.312$ a.m.u.) respectively.

The bulk densities (d_B) of all the samples were measured using Archimedes principle. The values of bulk density are reported in table 1. It is found that bulk density decreases with increase in magnesium content x . The bulk density d_B is less than X-ray density d_x . The small difference between these two density values is due to the existence of inter and intra granular porosity of the samples.

The values of X-ray density, bulk density were used to obtain percentage porosity of all the samples in the following equation [16];

$$p = 1 - \frac{d_b}{d_x} \quad \dots(4)$$

where, d_b is the bulk density and d_x is the X-ray density.

The porosity of the both the samples are given in table 1.

The crystallite size of all the samples was calculated using Debye-Scherer's formula as given below [16]. The plane (311) with maximum intensity was considered for full width at half maxima (FWHM), the obtained values of crystallite size given in table 1 suggests that the prepared samples have nanocrystalline nature.

$$t = \frac{0.9\lambda}{\beta \cos \theta} \quad \dots(5)$$

where, λ is wavelength of the Cu-K α radiation, β is the full width of the half maximum and θ is Bragg's angle. The average particle size shown in table 1.

Table 1: Lattice parameter (a in \AA), X-ray density (d_x in gm/cm^3), Bulk density (d_B in gm/cm^3), Porosity (P %), Unit cell volume (V), Average particle size (t in nm) and Grain size (G in nm) of $Co_{1-x}Mg_xFe_2O_4$ system (for $x=0.0$ and 0.25)

x	a	d_x	d_B	P	V	t	G
0.0	8.389	5.279	3.10	16.59	590.38	12.43	45
0.25	8.381	5.236	3.20	18.30	588.67	31.81	66

3.2 Fourier Transform Infrared Spectroscopy (FTIR)

The FTIR spectrum of the sintered $Co_{1-x}Mg_xFe_2O_4$ ferrite system (For $x = 0.0$ and 0.25) are shown in fig. 2 (a) and (b) respectively. The IR spectrum show the two principle absorption bands in the range of 400 cm^{-1} to 1000 cm^{-1} , the first absorption band is seen at around 436.93 cm^{-1} and second band is around 617.24 cm^{-1} for pure cobalt ferrite sample. The prominent two peaks observed in the FTIR spectra indicate the

formation of spinel ferrite. In the present study the absorption bands of all the ferrites under investigations are found to be in the reported range.

The absence of hydroxyl group, carboxylic group (at $3200 - 3700 \text{ cm}^{-1}$) in samples sintered at $550 \text{ }^\circ\text{C}$ for 4 h reveals the completion of chemical reaction.

The vibrational frequencies depend on the cation mass, cation oxygen distance and bonding force. Waldron and Hafner studied the vibrational spectra of various spinel ferrites and attributed them to intrinsic vibrations [17, 18].

The absorption bands (ν_1 and ν_2) correspond to intrinsic lattice vibrations of octahedral and tetrahedral coordination compounds in the spinel structure, respectively. The difference in frequency between the characteristic vibrations ν_1 and ν_2 may be attributed to the long bond length of oxygen - metal ions in the tetrahedral sites. Using the values of ν_1 and ν_2 , force constant (K_t and K_o) were computed.

Force constants K_0 and K_t have been obtained using the following relations:

$$K_t = 7.62 \times M_A \times \nu_1^2 \times 10^{-3} \quad \dots(6)$$

$$K_o = 10.62 \times \frac{M_B}{2} \times \nu_2^2 \times 10^{-3} \quad \dots(7)$$

The values of ν_1 and ν_2 and K_t and K_o are given in table 2 similar IR spectra has been reported in the literature [19, 20].

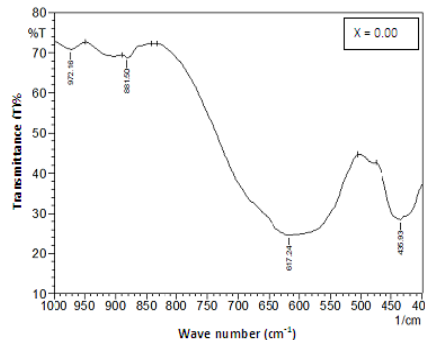


Fig. 2 (a): IR Spectrum of the system $Co_{1-x}Mg_xFe_2O_4$ ferrite system for $x = 0.0$

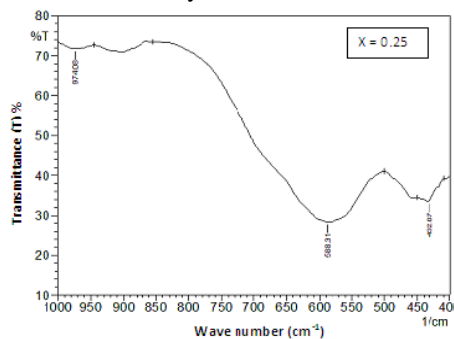


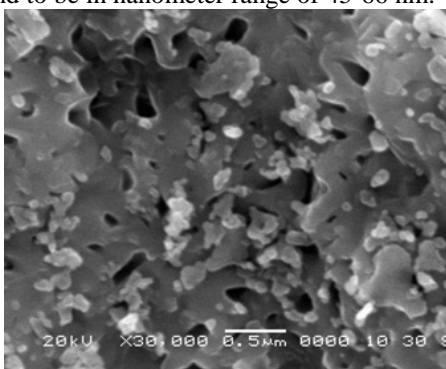
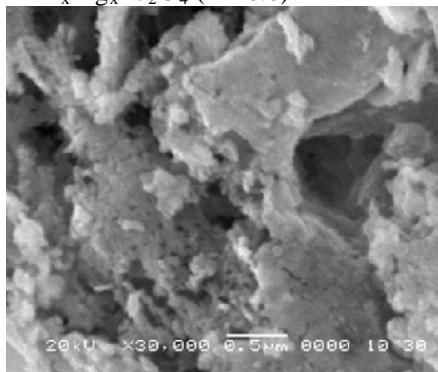
Fig. 2 (b): Spectrum of the system $Co_{1-x}Mg_xFe_2O_4$ ferrite system for $x = 0.25$

Table 2: Vibration band frequencies (ν_1 and ν_2) and force constant (K_t and K_0) of the system $\text{Co}_{1-x}\text{Mg}_x\text{Fe}_2\text{O}_4$ (for $x = 0.0$ and 0.25)

Comp. x	ν_2 (cm^{-1})	ν_1 (cm^{-1})	Force constant	
			$K_0 \times 10^5$	$K_t \times 10^5$
0.00	617.2	435.9	1.118	0.984
0.25	588.3	432.1	1.266	1.076

3.3 Scanning Electron Microscope

Figure 3 (a-b) shows morphological pattern of the prepared magnesium substituted cobalt spinel ferrite nanoparticles taken by scanning electron microscope (SEM). Evidently, from SEM images of the sintered magnesium substituted cobalt spinel ferrite samples it was seen that the morphology of the particles were almost spherical in shape, but agglomerated to some extent due to the interaction between magnetic nanoparticles. It can be observed that grains of uniform size are distributed throughout the surface which exhibits decreasing trend together with magnesium substitution. The particles size decreases significantly with increasing magnesium concentration since the ionic radius of magnesium is smaller than that of cobalt. The formation of nano size crystallites was confirmed through SEM images. The average grain size calculated from linear intercept method was found to be in nanometer range of 45-66 nm.


 Fig. 3 (a): SEM image of $\text{Co}_{1-x}\text{Mg}_x\text{Fe}_2\text{O}_4$ ($x = 0.0$)

 Fig. 3 (b): SEM image of $\text{Co}_{1-x}\text{Mg}_x\text{Fe}_2\text{O}_4$ ($x = 0.25$)

4. Conclusions

The nanocrystalline $\text{Co}_{1-x}\text{Mg}_x\text{Fe}_2\text{O}_4$ ($x = 0.0$ and 0.25) successfully synthesized by sol-gel auto combustion technique using AR grade metal nitrates and citric acid as a fuel. The X-ray diffraction results for the samples of $\text{Co}_{1-x}\text{Mg}_x\text{Fe}_2\text{O}_4$ ($x = 0.0$ and 0.25) showed the formation of single phase cubic spinel structure. The lattice constant is found to decrease with increasing Mg^{2+} concentration. The particle size of the samples calculated using the Debye Scherrer's formula was obtained in the range of 12-32 nm. Infrared spectra exhibit two distinct absorption bands near 600 cm^{-1} and 400 cm^{-1} indicating the characteristic features of spinel ferrites. The average grain size determined from scanning electron microscopy technique is of the order of 45 - 66 nm.

References

- [1]. J.Roelofs, A.Van Dillen, Y. K. de Jong, Catal. Today 60 (2000) 297-303
- [2]. V.Rives, O.Prieto, A.Dubey, S.Kannan, J. Catal. 220 (2003) 161-167.
- [3]. F.Prinetto, D.Tichit, R.Teissier, B.Coq, Catal. Today 55 (2000) 103-116.
- [4]. S.Murcia-Mascaros, R.Navarrao, L.Gomez-Sainero, U.Costantio, M. Nocchetti, J. L. G.Fierro., J. Catal. 198 (2001) 338-347.
- [5]. L.B.Kong, Z.W.Li, G.Q.Lin, Y.B.Gan, J. Amer. Cer. Soc. 90 (2007) 2104.
- [6]. Y.Konseoglu, H.Kavas, B.Aktas, Phys. Stat. Sol. A 203 (2003) 1595.
- [7]. J.F.Hochepped, M.P.Pileni, J. Appl. Phys. 87 (2000) 2472.
- [8]. M.H.Khedr, A.A.Omar, M.I.Nasr, E.K.Sedeek, J. Anal. Appl. Pyroly. 76 (2006) 203.
- [9]. S.Sarkar, C.Bansal, R.Nagarajan, Condens. Matter 3 (2002) 207095.
- [10]. L.J.Zhao, Q.Jiang, J. Magn. Mater. 322 (2010) 2485.
- [11]. M.Manjurul Haque, M.Huq, M.A.Hakim, Physica B 404 (2009) 3915.
- [12]. A.Goldman, Modern Ferrite Technology (New York, Marcel Dekker, 1993).
- [13]. S.H.Keluskar, R.B.Tangsali, G.K.Naik, J.S.Budkuley, J. Magn. Mater. 305, 296 - 303 (2006).
- [14]. S.G.Algude, S.M.Patange, S.E.Shirsath, D.R.Mane, K.M.Jadhav, J. Magn. Mater. 350 (2014) 39-41.
- [15]. Nalla Somaiah, T.V.Jayaraman, P.A.Joy, Dibakar Das, J. Magn. Mater. 324:14 (2012) 2286-2291.
- [16]. Elements of X-ray diffraction by B.D.Cullity, 1956 Addison-Wesley, publishing company, Inc.
- [17]. R.A.Waldron, Ferrites; An Introduction For Microwave Engineers, 1961.



- [18]. S.Hafner, F.Z.Laves, *Krist.* 115 (1961) 331.
- [19]. D.S.Mathew, R.S.Juang, *Chem. Eng. J.* 129 (2007) 51.
- [20]. S.Wells, C.V.Ramana, *Ceram. Int.* 39 (2013) 9549.